Non-linear compression with octupoles for current profile shaping

LCLS-II-TN-20-05

7/28/20

N. Sudar, K. Bane, Y. Ding, Y. Nosochkov and Z. Zhang

SLAC, Menlo Park, CA 94025, USA

Abstract:

In this technical note we present a method for controlling the higher order compression in the LCLS-II bunch compressors. An octupole magnet embedded in a chicane provides additional U5666, allowing for suppression of current horns and additional shaping of the electron beam current profile. By adjusting the octupole field strengths and electron beam betatron phase advance between octupoles embedded in subsequent bunch compressors, projected emittance growth from the first octupole is corrected.

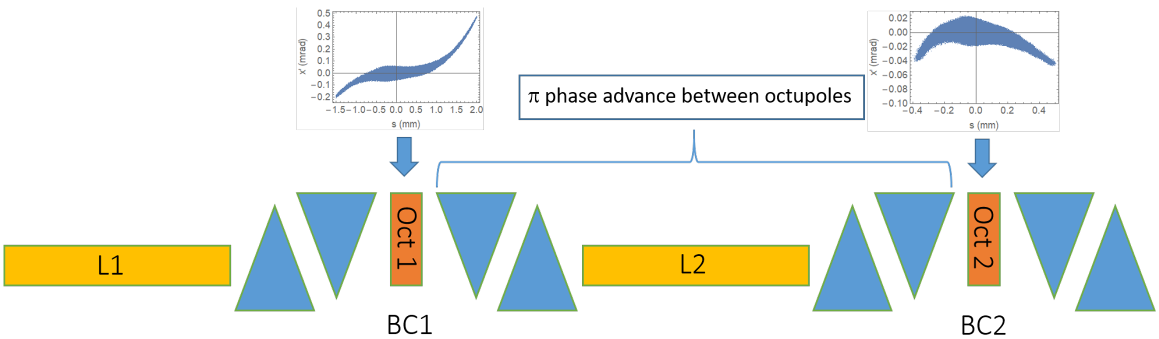

Figure 1: Basic layout of the proposed scheme

1 Introduction

In order to achieve the electron beam peak current required by many applications, high brightness linear accelerators employ multistage bunch compression. However, the peak current is limited by detrimental higher order compression from RF curvature, longitudinal space charge (LSC), coherent synchrotron radiation (CSR), and longitudinal wakefields. Although second order compression is typically compensated with a harmonic cavity [1], higher order compression often remains unchecked. This can lead to the production of horns in the current profile as the head and/or tail are over-compressed. These current horns can produce significant LSC modulation, CSR and longitudinal wakefields downstream, causing energy spread and projected emittance growth. This is particularly problematic in the LCLS-II linac where the electron beam must be transported from the Linac exit through a 2 km bypass line.

We present here a scheme for controlling the higher order compression, effectively suppressing current horns while providing additional knobs for shaping the current profile. An octupole magnet placed in a bunch compressor at a point of high transverse dispersion will provide a transverse kick correlated with z^3. After transport through the remainder of the bunch compressor, this kick is converted to third order compression, adjusting the U5666 of the bunch compressor. This scheme was investigated in [2-4], showing effective suppression of current horns. However, significant octupole strength will lead to growth of the projected emittance as the z dependent transverse kick will remain after compression. By installing a second octupole in a downstream bunch compressor, this kick can be compensated, while providing additional U5666, provided that the betatron phase advance and second octupole strength are chosen such that the kick is equal and opposite, Figure 1.

This scheme has been studied for the LCLS-II superconducting linac. Elegant [5] simulations of several potential configurations are shown with an incoming electron beam from injector simulations using a cathode laser with flattop and Gaussian temporal profile, section 2 and 3. A more detailed discussion of the longitudinal shaping scheme and emittance correction is presented in section 4 and 5 respectively. A discussion of minimization of particle losses after the first octupole is given in section 6.

2 Cathode laser with flattop temporal profile

For the case where the electron beam is produced by a cathode laser with a flattop temporal profile, current horns will naturally occur due to the third order chirp acquired in the injector and downstream collective effects. In order to study the proposed scheme we consider an initial distribution generated by Impact simulations of the LCLS-II injector [6-8]. Initial beam parameters are given in Table 1. The longitudinal phase space at the entrance of the first linac section is shown in Figure 2 for 100pC and 50 pC beams. Note that, according to Elegant's convention, the head of the beam is on the left throughout.

Initial optimization of the linac configuration is done using the 1-d tracking code, Li-Track [9]. Here the bunch compressors are considered point like transformations, where the U5666 can be specified. Optimization in LiTrack is done to maximize the peak current while minimizing the ratio of the peak current to core current, giving a solution with a flat current profile. As transverse effects are not considered in LiTrack, the desired transformation of the current profile can be found considering adjustment of the U5666 at BC2 only. When migrating to Elegant this total U5666 is split between BC1 and BC2, adjusting the ratio to minimize emittance growth. We note here that Elegant simulations are done considering BC1 and BC2 to have the same bend direction, calling for a π betatron phase advance for simplicity.

Table 2 gives Elegant simulation parameters for 4 configurations, cases I-III with 100pC and IV with 50 pC. Here the octupole ratios are chosen to minimize the projected emittance over the full beam. These ratios could be chosen to minimize the projected emittance only over the core of the beam current.

Table 1: Initial beam parameters flattop

Parameters	Value	
Energy (MeV)	100	100
Laser heater ΔE (keV)	5	15
Electron beam charge (pC)	100	50
Peak current (A)	13.2	9.4
Proj. emittance (mm-mrad)	0.3	0.17

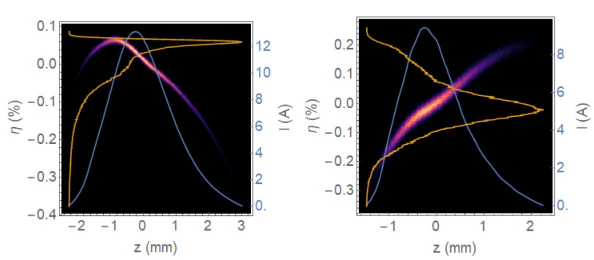

Figure 2: electron beam longitudinal phase at entrance of L1, showing current profile (blue) and energy distribution (yellow) for 100 pC (left) and 50 pC (right)

Given values for the BC1 and BC2 R_{56} and U_{5666} are found from simplified analytical expressions. The corresponding longitudinal phase spaces at the end of BC2 and hard x-ray undulator entrance are shown in Figure 3.

Although emittance growth is well compensated after BC2, the proposed scheme is still limited by particle losses in the collimator immediately downstream of BC1 due to strict radiation requirements. Case I gives a configuration where losses are kept below 1% at the sacrifice of both horn suppression and emittance compensation. For case II and III we assume that increased upstream energy collimation or running at lower repetition rate could reduce losses to an acceptable level, focusing on achieving a flat, high peak current profile ideal for self-seeding. Case IV shows that with the decreased initial bunch length for the 50 pC case a configuration with no losses can be found. In all cases, remnant projected emittance growth can be attributed to second order transverse focusing effects in the second linac section. However, the slice emittance in the core of the beam is unaffected. This is discussed further in section 5. Case II is used as an example case throughout the remainder of the text.

Table 2: Parameters for Elegant simulations with incoming beam from flattop temporal profile cathode laser

Parameter	Case I	Case II	Case III	Case IV
L1 (voltage per cavity [MV])	13.3879	13.5329	14.8525	15.625
L1 RF phase [degrees]	-22	-24.9	-24.9	-26.394
L1 harmonic cavity (volt per cavity [MV])	3.041	2.97771	3.23217	4.4969
L1 harmonic cavity RF phase [degrees]	-165.448	-167.074	-168.027	-163.117
Energy at BC1 [GeV]	0.25	0.25	0.265	0.260
L2 (voltage per cavity [MV])	16.181	16.0134	16.4413	15.2442
L2 RF phase [degrees]	-29.3966	-35.5773	-38.4953	-32.0556
Energy at BC2 [GeV]	1.6	1.5	1.5	1.5
L3 (voltage per cavity [MV])	15.0	15.6969	15.6969	15.6969
L3 RF phase [degrees]	0	0	0	0
Energy at undulator entrance [GeV]	4	4	4	4
BC1 R_{56} [mm] (BC1 compression, bend angle [mrad])	-51.25 (2.7, 99.42)	-47.447 (2.6, 95.66)	-47.594 (2.7, 95.81)	-31.13 (2.4, 77.49)
BC2 R_{56} [mm] (total compression, bend angle [mrad])	-53.843 (80.2, 51.25)	-44.925 (112, 46.81)	-41.034 (157, 44.74)	-44.457 (90, 46.57)
BC1 octupole K_3L (U_{5666} [m])	-2888.84 (2.253)	-5386.57 (3.670)	-5502.6 (3.775)	-2531.2 (0.699)
BC2 octupole K_3L (U_{5666} [m])	-468.92 (6.279)	-457.01 (4.244)	-446.0 (3.4465)	-334.1 (3.014)
I (undulator ent. [kA])	1	1.5	2	1
Proj. emittance (@undulator [mm-mrad])	1.05	0.84	0.96	0.38
Losses at BC1 collimator [%]	0.95	4.06	4.58	0.0

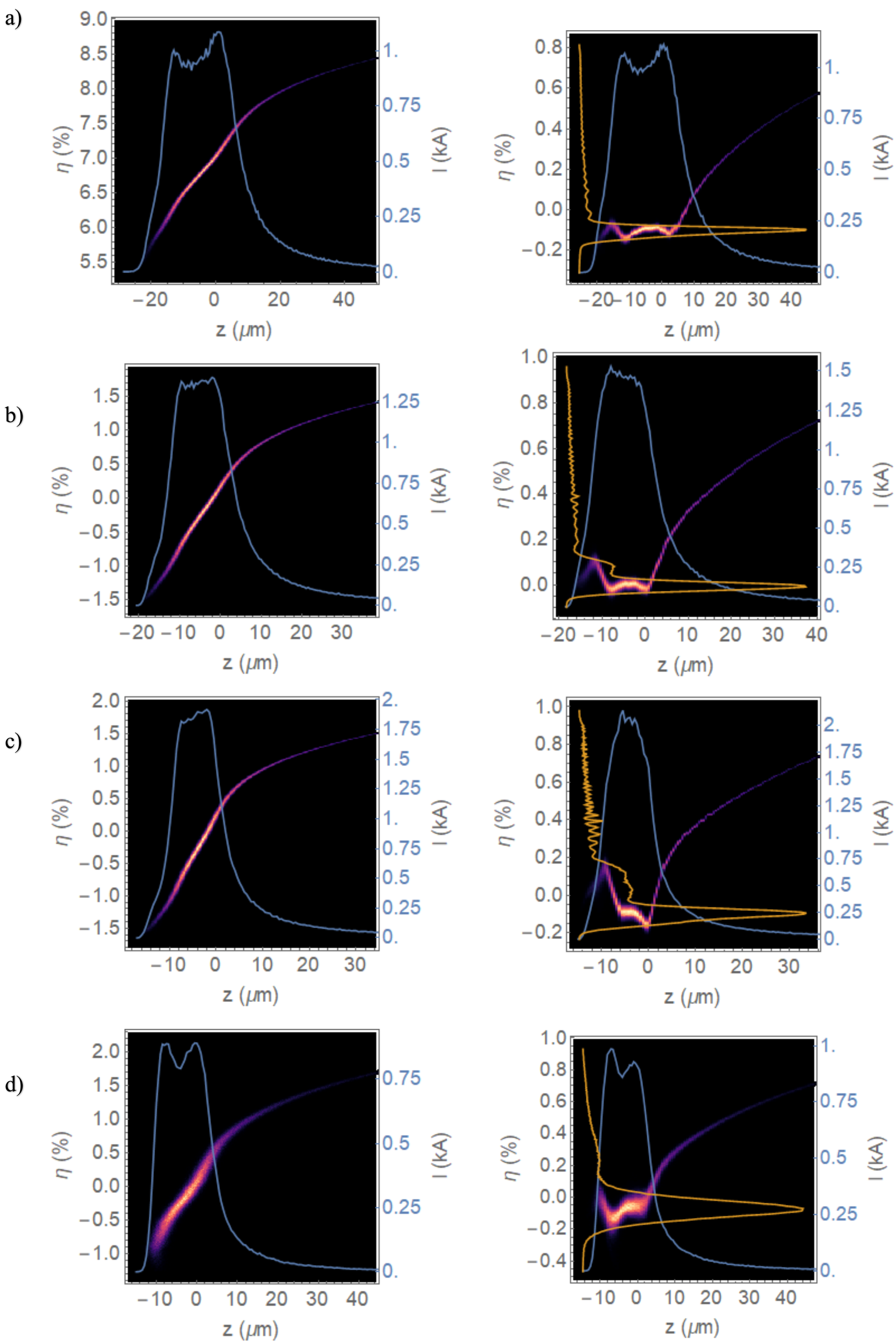

Figure 3: Longitudinal phase space from Elegant at the end of BC2 (Left) and start of the hard x-ray undulator (Right) for case I (a), case II (b), case III (c), and case IV (d). The current profile is shown in blue with the final energy distribution in yellow.

3 Cathode laser with Gaussian temporal profile

For the case where the electron beam is produced by a cathode laser with a Gaussian temporal profile, the initial current profile is peaked near the head of the beam, with significantly less third order chirp. This distribution will not generally lead to the growth of current horns after downstream compression, but the final current shape is typically asymmetric. Since in the LCLS-II configuration the longitudinal space charge and longitudinal wakefields in the long bypass line play an important role to reduce the remaining chirp after the final linac section, adjustment of higher order compression is still useful in shaping the current profile and modifying the final longitudinal phase space. We consider an initial distribution generated by Astra simulations of the LCLS-II injector [10]. Initial beam parameters are given in Table 3. The longitudinal phase space at the entrance of the first linac section is shown in Figure 4. To counteract the stronger micro-bunching instability, the amplitude of the laser heater modulation is increased to 7.5 keV. Whether this increased microbunching instability is a physical or statistical effect remains to be seen.

In order to increase and flatten the peak current while controlling the final longitudinal phase space, it is necessary to shift the current distribution peak towards the tail of the beam. This can be accomplished by adjusting second order compression with the harmonic linearizer, while increasing the nominal third order compression of the bunch compressors with the aid of the octupoles.

Table 4 again gives Elegant simulation parameters for 3 configurations. The corresponding longitudinal phase spaces at the end of BC2 and hard x-ray undulator entrance are shown in Figure 5. Case A gives a configuration where the current profile is ramped to produce a final longitudinal phase space with narrow energy spread. Case B gives a configuration with a flattened current profile at the exit of BC2 with a peak current of 2 kA. Case C gives a configuration with high peak current, but with a significant chirp at the undulator entrance. This could be potentially utilized with a chirped taper scheme in the FEL lasing process. None of these cases require a significant octupole kick and projected emittance growth after BC1 is small compared with the flat beam case. Projected emittance growth from CSR is reduced by adjusting the BC2 horizontal dispersion with quadrupoles inside BC2 [11]. None of the three cases exhibit particle losses due to the shorter incoming electron beam.

Table 3: Initial beam parameters

Parameters	**Value**
Energy (MeV)	92.36
Laser heater ΔE (keV)	7.5
Electron beam charge (pC)	100
Peak current (A)	10.76
Projected emittance (mm-mrad)	0.5

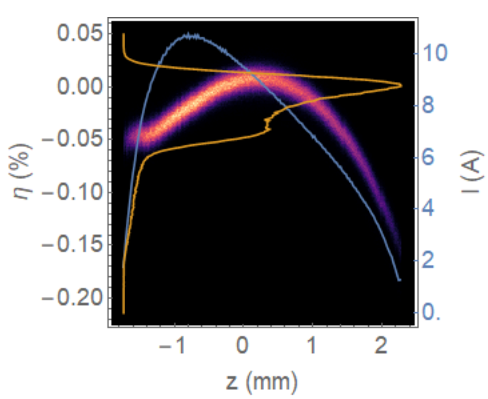

Figure 4: electron beam longitudinal phase at entrance of L1, showing current profile (blue) and energy distribution (yellow)

Table 4: Parameters for Elegant simulations with incoming beam from Gaussian temporal profile cathode laser

Parameter	Case A	Case B	Case C
L1 (voltage per cavity [MV])	15.4023	13.7818	16.0166
L1 RF phase [degrees]	-24.2386	-24.9	-32.0846
L1 harmonic cavity (voltage per cavity [MV])	3.75	2.6701	3.71931
L1 harmonic cavity RF phase [degrees]	-172.246	-179.473	-181.318
Energy at BC1 [GeV]	0.258	0.25	0.265
L2 (voltage per cavity [MV])	16.0	15.0712	15.9439
L2 RF phase [degrees]	-33.9127	-30.2109	-35.2267
Energy at BC2 [GeV]	1.532	1.5	1.5
L3 (voltage per cavity [MV])	15.6969	15.6969	15.6969
L3 RF phase [degrees]	0	0	0
Energy at undulator entrance [GeV]	4.03	3.99	4
BC1 R_{56} [mm] **(BC1 compression factor, bend angle [rad])**	-52.45 (3.3, 0.10058)	-70.695 (3.66, 0.11677)	-48.525 (3.33, 0.09674)
BC2 R_{56} [mm] **(total compression factor, bend angle [rad])**	-43.415 (152, 0.04602)	-50.554 (171, 0.04966)	-41.266 (286, 0.04487)
BC1 octupole K_3L **(U_{5666} [m])**	365.09 (-0.417)	900 (-1.538)	335.24 (-0.342)
BC2 octupole K_3L **(U_{5666} [m])**	73.02 (-0.734)	212.8 (-2.657)	70.14 (-0.644)
I (undulator ent. [kA])	1.6	2.0	3.5
Proj. emittance (undulator ent. [mm-mrad])	0.65	0.74	0.87
Losses at BC1 collimator [%]	0.0	0.0	0.0

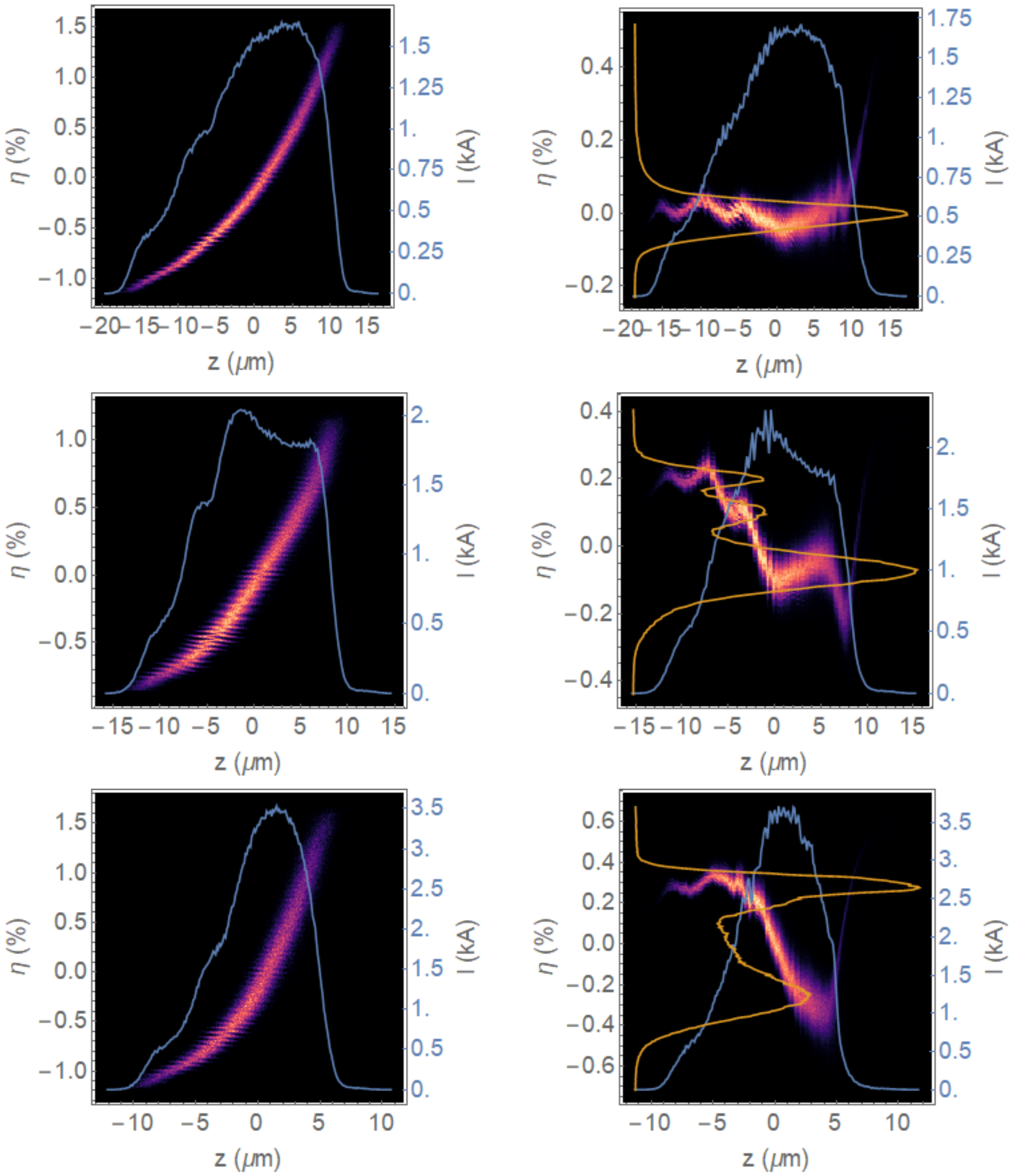

Figure 5: Longitudinal phase space from Elegant at the end of BC2 (Left) and start of the hard x-ray undulator (Right) for case A (top), case B (middle) and case C (bottom). The current profile is shown in blue with the final energy distribution in yellow.

4 Longitudinal shaping

An electron passing through an octupole magnet with negligible vertical offset relative to the magnetic center, will receive a horizontal kick depending on its horizontal offset given by:

$$x' \sim -\frac{B'''}{6B\rho} L_0 x^3 \equiv -\frac{1}{6} K_3 L_0 x^3 \qquad (1)$$

Here L_0 is the octupole length and K_3 is the octupole's geometric strength. Placing an octupole at a point of high transverse dispersion, we assume an electron's transverse offset at the octupole entrance is dominated by its energy offset from the central energy. Considering placing the octupole in the center of a chicane, the transverse offset at the octupole entrance is then given by the R_{16} from a simple dogleg, leading to an energy dependent kick:

$$x_{oct} = R_{16}\delta \sim -\theta(l_b + l_d)\delta \rightarrow x'_{oct} = \frac{1}{6} K_3 L_0 \theta^3 (l_b + l_d)^3 \delta^3 \qquad (2)$$

Here l_b is the dipole length, l_d is the drift length and θ is the bend angle associated with the chicane. After transport through the remainder of the chicane, the resultant path length difference from the octupole kick is given by the R_{52} from a simple dogleg.

$$z_{foct} = R_{52} x'_{oct} = -\frac{1}{6} K_3 L_0 \theta^4 (l_b + l_d)^4 \delta^3 \qquad (3)$$

Considering the nominal approximate values for 1st, 2nd and 3rd order longitudinal dispersion from a chicane, including the octupole gives:

$$R_{56} \sim -2\theta^2 \left(l_d + \frac{2}{3} l_b\right), \ T_{566} \sim -\frac{3}{2} R_{56}, \ U_{5666} \sim -\frac{1}{6} K_3 L_0 \theta^4 (l_b + l_d)^4 + 2R_{56} \qquad (4)$$

We can gain some insight into the role of higher order compression in the growth and suppression of current horns by considering the transformation of the initial current profile in the limit of zero initial energy spread. For an initial current profile, $I_0(z_0)$, transport through a dispersive element, $z_1 = z_0 + f(z_0)$, gives a final current:

$$I_1(z_1) \sim \left(\frac{\partial z_1}{\partial z_0}\right)^{-1} I_0[z_0(z_1)] \sim C_1 * (1 + c_{11} z_0(z_1) + c_{12} z_0(z_1)^2 + \cdots)^{-1} * I_0[z_0(z_1)] \qquad (5)$$

$$C_1 \equiv \left(\left.\frac{\partial z_1}{\partial z_0}\right|_{z_0=0}\right)^{-1}, \quad c_{11} \equiv C_1 * \left(\left.\frac{\partial^2 z_1}{\partial z_0^2}\right|_{z_0=0}\right), \quad c_{12} \equiv \frac{1}{2} C_1 * \left(\left.\frac{\partial^3 z_1}{\partial z_0^3}\right|_{z_0=0}\right)$$

From the above expression we see that if the contribution from higher order compression approaches zero within the initial current profile, current horns can form. This can be avoided by adjusting the second order chirp and U_{5666} to reduce the 2nd and 3rd order compression terms, c_{11} and c_{12}. Perhaps more importantly, values for c_{11} and c_{12} can be found that give a desired current profile without giving rise to current horns. Maintaining values for the higher order compression terms, the linac parameters can be varied and the peak current can be scaled by the overall compression factor, C_1, while approximately maintaining the current profile, considering only the linear transformation of z:

$$z_0(z_1) \sim C_1 * z_1 \equiv \zeta \rightarrow I_1(\zeta) = C_1 * (1 + c_{11}\zeta + c_{12}\zeta^2)^{-1} I_0[\zeta] \qquad (6)$$

As stated earlier, initial optimization of the final current profile was done in the 1-d tracking code LiTrack and confirmed with Elegant. Given linac parameters from this optimization, the initial electron beam chirp, and linac wakefields calculated analytically from [12], a simple model can be considered keeping terms up to 3rd order. Provided that current horns are suppressed, CSR and longitudinal space charge can be ignored. For case II, this analysis gives values for the higher order compression terms, c_{11} = 1.42 and c_{12} = 25051.7 after BC1, and c_{11}= 985.6 and c_{12} = 624007 after BC2. If the current profile after BC1 is approximately maintained then the linac wakefields in L2 can be scaled with the BC1 compression factor, and the parameter space can be explored further while maintaining the final current profile. Figure 6 shows comparison of the various simulation methods for case II as an example. The same configuration with octupoles removed is shown for reference.

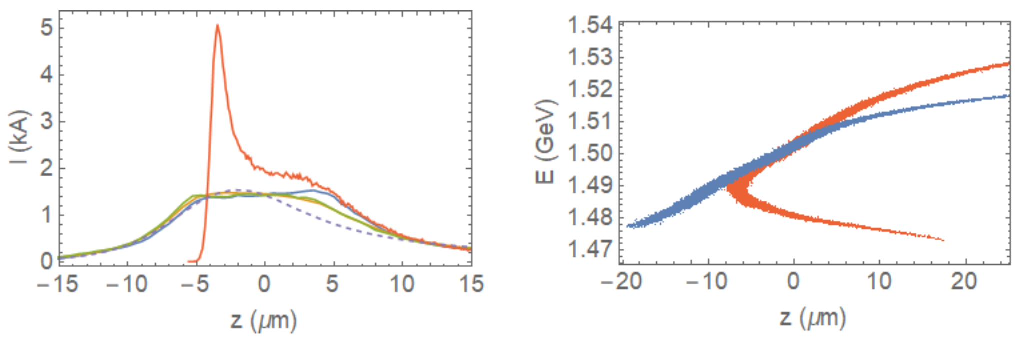

Figure 6: Left: current profile from LiTrack (green), Elegant (blue), Elegant with octupoles off (red), simplified transformation to 3rd order (yellow), and current transformation from equation 5 (dashed). Right: comparison of longitudinal phase space from Elegant with octupoles on (blue) and off (red)

5 Emittance correction

As mentioned earlier the double-octupole scheme is used to correct projected emittance growth from the transverse kick associated with a single octupole. In order to better understand the emittance compensation scheme we can approximate the transverse kick from the two octupoles at pertinent locations. The expression from equation 2 can be written in terms of the beam coordinate in the limit that δ is dominated by the correlated chirp. At BC1 the linear chirp depends on the initial chirp, linac wakefields, harmonic linearizer and RF phase. However, we can express this chirp in terms of the BC1 compression factor, C_1, and the chicane bending angle, θ_1.

$$x'(z) = \frac{1}{6} K_1 L_1 \left(\frac{l_{d1}+l_{b1}}{l_{d1}+\frac{2l_{b1}}{3}}\right)^3 \left(\frac{1}{\theta_1}\right)^3 \left(\frac{C_1-1}{C_1+1}\right)^3 z^3 \qquad (7)$$

Here K_1 refers to the geometric strength of the first octupole and L_1 is the octupole length, l_{b1} is the chicane magnet length and l_{d1} is the chicane drift length. It should be noted that z refers to the transformed beam coordinate after transport through half of the BC1 chicane, Figure 7a.

After transport through the subsequent linac section, assuming the electron beam goes through an n*π betatron phase advance, we can write the transformation of the first octupole kick at the entrance of the second octupole in terms of the energy and beta function at the BC1 octupole, E_1 and β_1, and energy and beta function at the BC2 octupole, E_2 and β_2.

$$x'(z) = -(-1)^n \frac{1}{6} K_1 L_1 \left(\frac{l_{d1}+l_{b1}}{l_{d1}+\frac{2l_{b1}}{3}}\right)^3 \left(\frac{1}{\theta_1}\right)^3 \left(\frac{C_2*(C_1-1)}{C_2+C_1}\right)^3 \sqrt{\frac{\beta_1 E_1}{\beta_2 E_2}}\, z^3 \qquad (8)$$

Again the octupole kick is written in terms of the compressed longitudinal beam coordinate after transport through half of the BC2 chicane in terms of the total compression factor, C_2, Figure 7b.

The kick provided by the second octupole can again be written expressing the linear chirp at the BC2 entrance in terms of the BC1 and total compression factors. If the bend direction of the BC2 chicane is opposite to that of BC1 then the sign of this kick will flip:

$$x'(z) = -\frac{1}{6} K_2 L_2 \left(\frac{l_{d2}+l_{b2}}{l_{d2}+\frac{2l_{b2}}{3}}\right)^3 \left(\frac{1}{\theta_2}\right)^3 \left(\frac{C_2-C1}{C_2+C_1}\right)^3 z^3 \qquad (9)$$

Here K_2 refers to the geometric strength of the second octupole, L_2 is the octupole length, l_{b2} is the chicane magnet length, l_{d2} is the chicane drift length, and θ_2 is the chicane bend angle, Figure 7c. Setting the total kick to zero, given by the sum of equations 8 and 9, gives an approximate condition on the ratio of octupole strengths for correcting the projected emittance growth.

$$\frac{K_2 L_2}{K_1 L_1} = \left(\frac{(l_{d1}+l_{b1})*\left(l_{d2}+\frac{2l_{b2}}{3}\right)}{(l_{d2}+l_{b2})*\left(l_{d1}+\frac{2l_{b1}}{3}\right)}\right)^3 \left(\frac{\theta_2}{\theta_1}\right)^3 \left(\frac{C_2*(C_1-1)}{C_2-C_1}\right)^3 \sqrt{\frac{\beta_1 E_1}{\beta_2 E_2}} \qquad (10)$$

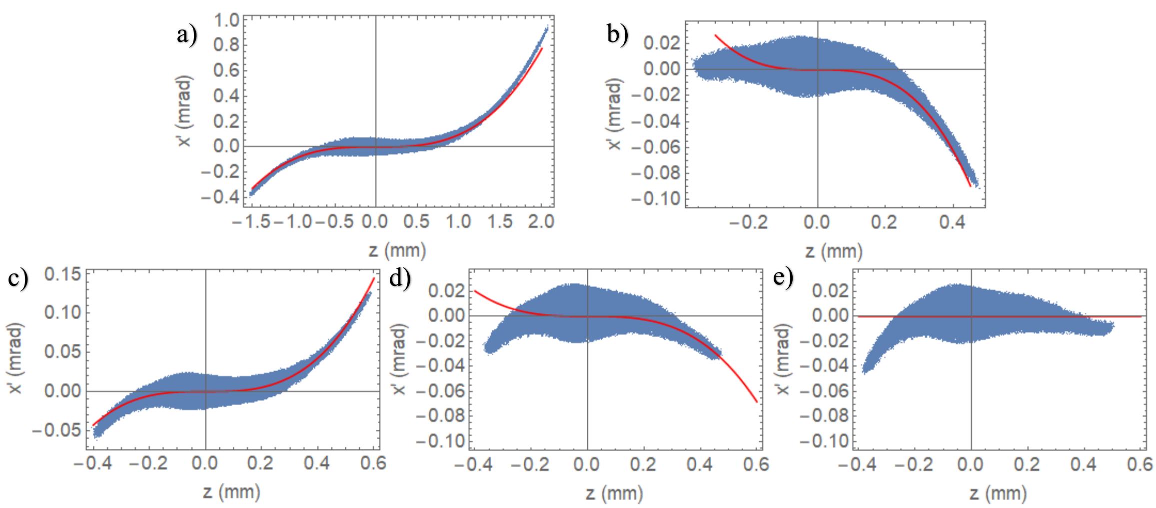

Figure 7: (a) Kick after BC1 octupole. (b) BC1 octupole kick transported to BC2 octupole entrance. (c) BC2 octupole kick with BC1 octupole off. (d) Combined kick from BC1 and BC2 octupole with minimized projected emittance. (e) Combined octupole kick with analytically calculated projected emittance minimized. Analytical estimates are shown in red.

A more detailed discussion of the emittance correction scheme can be found in [13]. Figure 7d shows the corrected octupole kick after varying K_2/K_1 to minimize the projected emittance in Elegant simulations for the case II configuration. Here we see that additional emittance growth in the head of the beam, possibly from CSR, gives an optimal K_2/K_1 ratio differing from that given by the above analysis. Figure 7e shows the residual kick with the K_2/K_1 ratio given by equation 10, noting that for this configuration, $\beta_1/\beta_2 \sim 1/3$.

Varying the K_2/K_1 ratio while maintaining the total U_{5666}, we see the slice emittance after BC2 is preserved in the core of the beam, varying only in the head of the beam. Varying the betatron phase advance between octupoles, again the core slice emittance is preserved, however there is more significant change in the head. This could possibly mitigated by properly optimizing the lattice for each case, Figure 8.

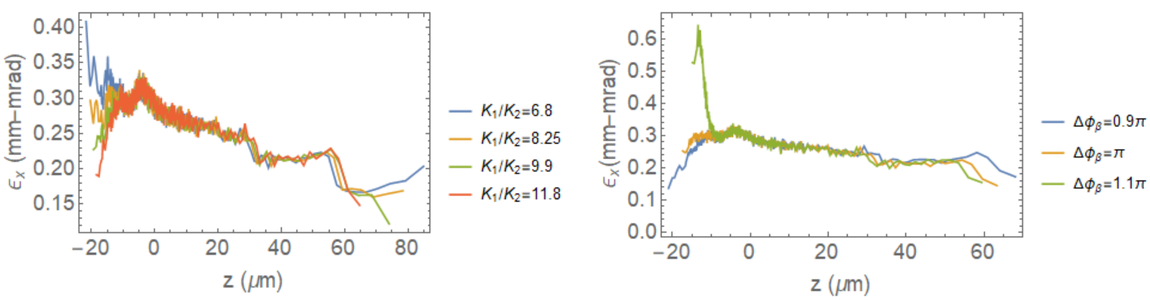

Figure 8: (Left) Slice emittance at BC2 exit varying the ratio between BC1 and BC2 octupole strengths. (Right) Slice emittance varying the betatron phase advance between BC1 and BC2 octupoles.

6 Particle losses

For the high power LCLS-II facility, we have several groups of halo collimator systems to remove the dark current. As stated earlier, in the example of the 100 pC flattop laser case, we observed particle losses at the collimator located downstream of BC1. Figure 9 shows the location of particles in the incoming phase space that will be collimated for the case II configuration. From this we see that a significant portion of these lost particles could potentially be truncated earlier using an upstream energy collimator in the laser heater area where the energy is still low. As seen in case IV of Table 2, this is also accomplished by reducing the beam charge, in turn reducing the initial bunch length.

Losses can also be reduced by adjusting the linac configuration. Again using case II as an example, we can vary the BC1 energy, chirp and R_{56} to minimize the BC1 octupole kick given by equation 7. This is done while maintaining the total compression after BC2 and higher order compression terms given by equation 5, to ensure that the final current profile is maintained. The emittance correction condition given by equation 10 is also maintained.

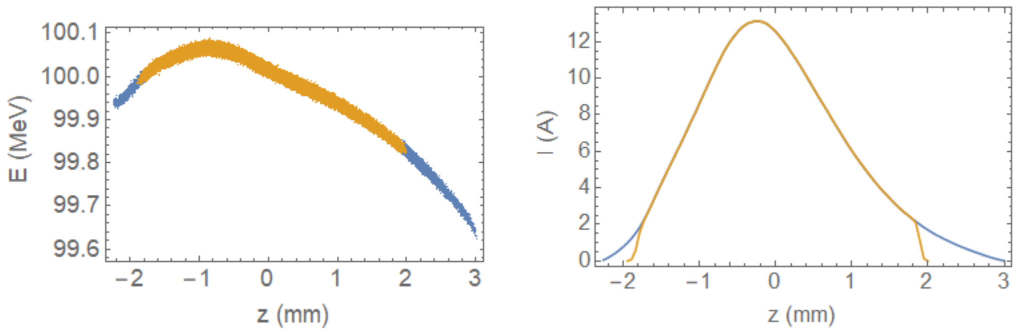

Figure 9: (Left) Longitudinal phase space at beginning of L1 linac (blue) showing particles transported through collimators (yellow). (Right) current profile at beginning of L1 (blue) showing current profile of non-collimated particles (yellow).

Figure 10 shows the octupole kick, normalized to the kick associated with case II, for BC1 energy 230 MeV, 250 MeV and 270 MeV. Solutions with linac parameters outside of LCLS-II specifications are cut. From this we see a general trend that the BC1 kick is reduced for larger chirp, smaller R56, and larger BC1 energy. Elegant simulations with the solution giving minimal kick, show reduction of particle losses to ~3%. This could possibly be reduced further at the expense of some horn suppression and emittance correction, as is shown in case I of Table 2.

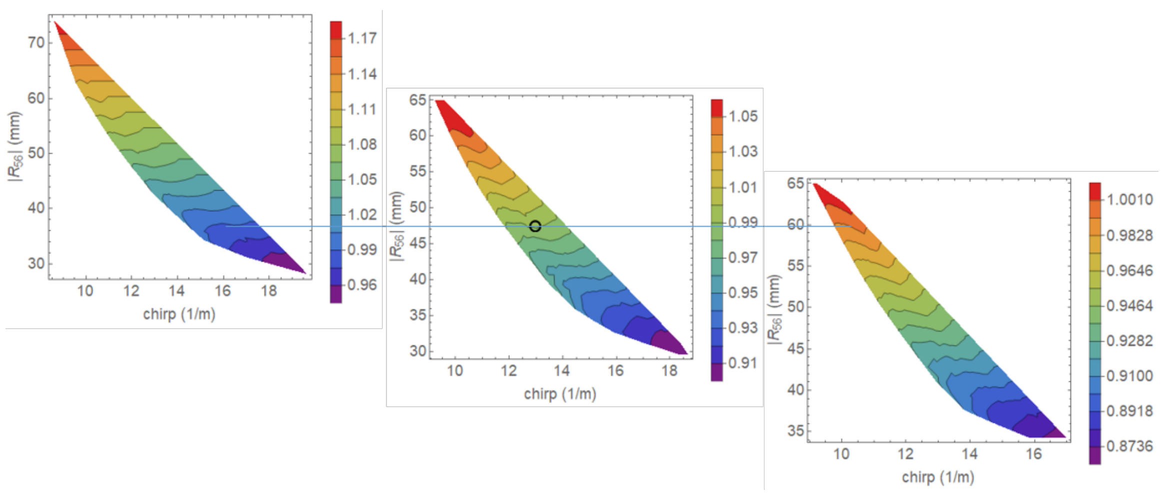

Figure 10: BC1 octupole kick normalized to the octupole kick associated with case II, varying the BC1 R56 and electron beam chirp at the BC1 entrance for BC1 energy 230 MeV (left), 250 MeV (center) and 270 MeV (right). For reference the point associated with case II is indicated by the black circle. Plots are offset vertically to align where the normalized kick = 1 for each energy.

7 Further discussion/conclusions

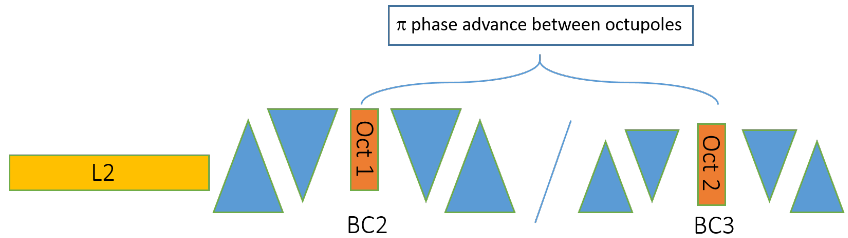

Figure 11: Double chicane configuration with pi phase advance (not shown)

Initial studies of the presented scheme considered a second smaller chicane installed immediately downstream of BC2, Figure 11. This setup simplifies the scheme as there is no energy gain or collimation between the two octupoles and was considered at one point for suppression of CSR effects [14]. However, the space required for the betatron phase advance and additional chicane is not realizable in the current LCLS-II configuration.

Reference:

[1] P. Emma, Reports No. SLAC-TN-05-004, No. LCLS-TN01-1, (2001)

[2] http://accelconf.web.cern.ch/fel2019/papers/thp035.pdf

[3] https://journals.aps.org/prab/abstract/10.1103/PhysRevAccelBeams.19.104402

[4] https://journals.aps.org/prab/abstract/10.1103/PhysRevAccelBeams.20.030705

[5] M. Borland, "Elegant: A Flexible SDDS-Compliant Code for Accelerator Simulation," Advanced. Photon Source LS-287, (2000)

[6] G. Marcus and J. Qiang, Reports No. LCLS-II-TN-17-04, (2017)

[7] J. Qiang, R. D. Ryne, S. Habib, V. Decyk, An object-oriented parallel particle-in-cell code for beamdynamics simulation in linear accelerators, J. Comput. Phys. 163, (2000) p. 434.

[8] J. Qiang, S. Lidia, R. D. Ryne, and C. Limborg-Deprey, A three-dimensional quasi-static model for high brightnees beam dynamics simulation, Phys. Rev. ST Accel. Beams 9, (2006) 044204.

[9] K. Bane and P. Emma, in Proceedings of the 21st Particle Accelerator Conference, PAC2005, Knoxville, TN, 2005. (IEEE, Piscataway, NJ, 2005), p. 4266

[10] Astra, https://www.desy.de/~mpyflo/

[11] N. Neveu et al, Reports No. LCLS-II-20-03, (2020)

[12] https://journals.aps.org/prl/abstract/10.1103/PhysRevLett.120.014801

[13] Y. Nosochkov, Reports No. LCLS-II-20-04, (2020)

[14] http://inspirehep.net/record/469134/files/30014213.pdf?version=1 (chapter 7.4.1)